Surface and Coatings Technology, 47 (1991) 770–791

Superhard i-C coatings used in complex processes of surface strengthening of tools and machine parts

N. Novikov, V. Gorokhovsky and **B. Uryukov**
Institute for Superhard Materials of the Ukrainian S.S.R. Academy of Sciences, 2 Avtozavodskaya St., Kiev 252153 (U.S.S.R.)

Abstract

A study of the mechanical properties of i-C coatings deposited onto substrates of different materials indicated that the plastic strain of the substrate had a considerable effect on the measured values of microhardness and elastic modulus, and on the fracture toughness, fatigue strength and other mechanical properties of the coatings. These characteristics determine the efficient use of i-C coatings on tools and on friction surfaces of machines.

A greater effect of i-C coatings on the increase in wear resistance of tools and machine parts can be achieved at the expense of hardening the surface layer between the base of the machine part and the i-C coating. At the same time the surface strains are reduced and the contact resistance increases.

To ensure complex strengthening of tools and machine parts, a "Thermion" installation was developed. The automated modular complex allows ion-diffusion alloying (nitriding, carbonitriding and others) of metal substrates to a depth of up to 100 μm, the deposition of multilayer cermet coatings of up to 10 μm in thickness, and the deposition of a superhard i-C coating at both low ($T \lesssim 600$ °C) and high ($T \gtrsim 900$–1000 °C) substrate temperatures. The installation is the result of developments of a team including specialists from the Ukraine, Estonia, Belorussia, R.S.F.S.R., Poland, Romania and East Germany. The "Thermion" installation comprises a vacuum electric arc device in combination with a magnetron or electron-beam source used for evaporation, ionization, destruction and excitation of the substances deposited. In the process of ion-vacuum treatment, an r.f. voltage is applied to the substrate holder which ensures additional stimulation of plasma–chemical processes owing to a rise in electron temperature and a degree of discharge unbalance, and excludes break-through of the surface of the machine part treated by plasma. The potentials of the installation are shown by examples.

1. Introduction

Owing to their high hardness, tribological properties, abrasive wear resistance and anticorrosion properties [1–3], thin film metal–ceramic and superhard carbon coatings are now being used successfully for strengthening the surfaces of tools and machine parts. The efficiency of these coatings is directly related to their composition, structure, the method used to form the layers, which is dependent on the substrate material, and the conditions under which the strengthened parts are operated. Treatment of the surface layer of the parts before deposition of the final superhard layer may include thermodiffusion (annealing, oxidation, nitriding and others) and the deposition of several layers of different metal–ceramic coatings. During the complex processes of strengthening tools and machine parts from steel,

Elsevier Sequoia/Printed in The Netherlands

thermodiffusion of the surface layer is used to reduce critical stresses at the interface of the base material and the deposited coating [4]. In other cases it is necessary to modify the structure of the surface layer on the base to reduce the effects of defects and residual stresses, which result from the preliminary mechanical machining, and to clean and activate the base surface before deposition of the i-C coating.

The interlayers of metal–ceramic coatings must ensure high adhesion with both the substrate surface and the final superhard layer. Using an optimal combination of thermodiffusion method, interlayers and final superhard coating, a reduction in internal stresses, high fracture toughness and fatigue strength of the surface of the strengthened parts are achieved.

Because of the temperature constraints on tempering of steels and alloys from which most tools and machine parts used at present are manufactured, the complex strengthening processes are achieved using relatively low-temperature plasma vapour deposition methods, applied in combination with ion-vacuum and plasma-chemical processes under carefully controlled technological conditions. It is possible to realize all the basic stages of the technological process in one cycle; cleaning and modification of the surface, thermodiffusion treatment, deposition of interlayers of cermet coatings and deposition of the final layer of superhard carbon or similar material. The equipment developed to realize these processes must be able to be used to strengthen both small and large parts of complex shape, ensuring uniformity of thickness and properties of the coatings all over the treated surface.

2. Experimental techniques

Experimental studies of the complex technology of vacuum-plasma strengthening of tools and machine parts were carried out on a purposely developed modular complex "Thermion" which uses one cycle to accomplish the cleaning and modification of a surface, ion-diffusion saturation of the surface layer with nitrogen, carbon, silicon and other elements, deposition of multilayered metal, dielectric and cermet coatings of metal and refractory compounds, as well as those with amorphous and fine crystalline structure, and superhard i-C, i-BN and diamond coatings. The "Thermion" comprises a set of replaceable modules of energy source, permitting the installation structure to be modified according to the technology requirements [5]. One of the basic modifications of the complex is schematically shown in Fig.1.

The Thermion complexes are provided with cathode-arc, magnetron and electron-beam sources for the atomization of solid substances. The ionization and activation of plasma-forming gas and evaporated atoms are accomplished in the anode region of the low-pressure electric arc which enables a high degree of ionization to be used over practically the entire range of working pressures from 10^{-2} to 10^{-5} hPa. This also allows the range of working pressures of a highly productive r.f. magnetron source to be extended towards lower pressures (down to 5×10^{-5} hPa). Figure 2 shows the dependence of ion

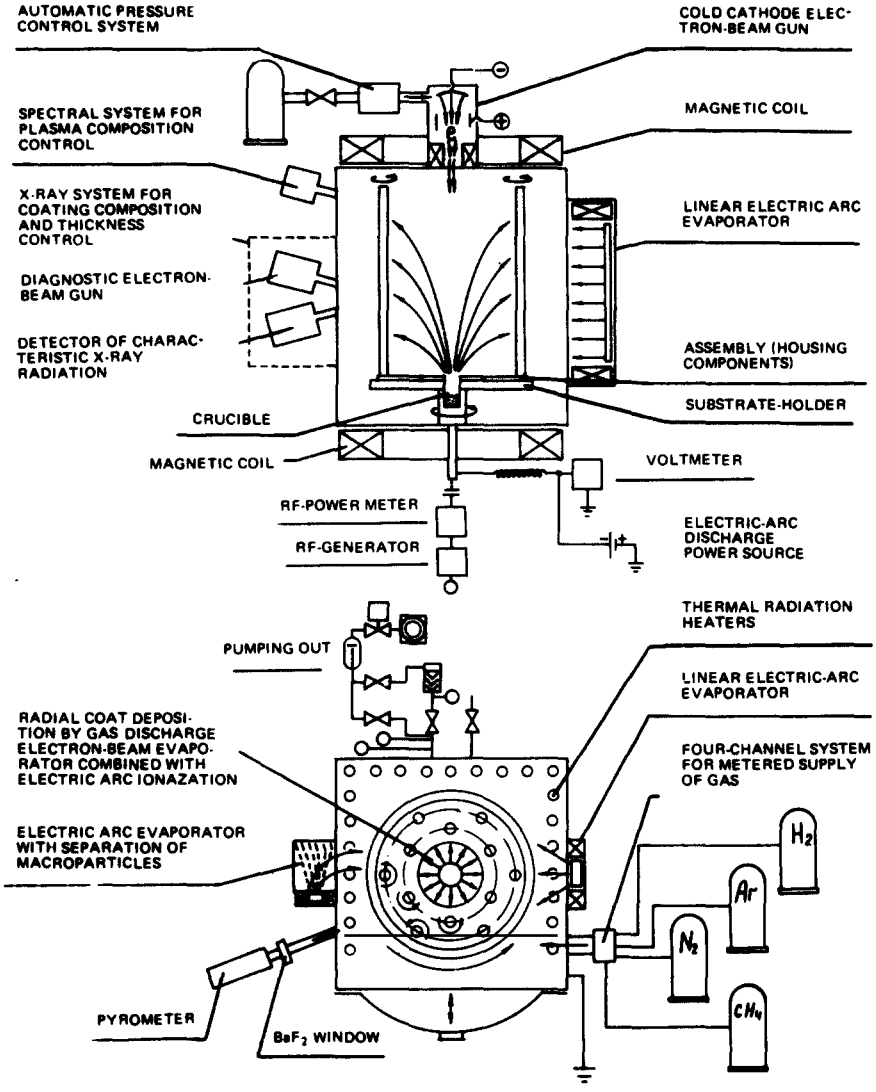

Fig. 1. A schematic representation of the modular complex Thermion-1.

flow to the collector, with a surface area $S_c = 800\ \text{cm}^2$ under a potential of 100 V placed in the anode region of the vacuum arc, on the current of the arc at different gas pressures. It is seen that at $P \lesssim 5 \times 10^{-4}$ hPa, the density of the ion flow to the collector may be as much as $10\ \text{mA cm}^{-2}$.

The uniformity of the ion-vacuum treatment of complex machine parts is achieved at the expense of the generation of a strongly ionized plasma cloud with magnetized electrons within the entire volume of the vacuum chamber ($\omega_e \tau_e \gg 1$). Such plasma spreads freely along the lines of the plasma-cloud-

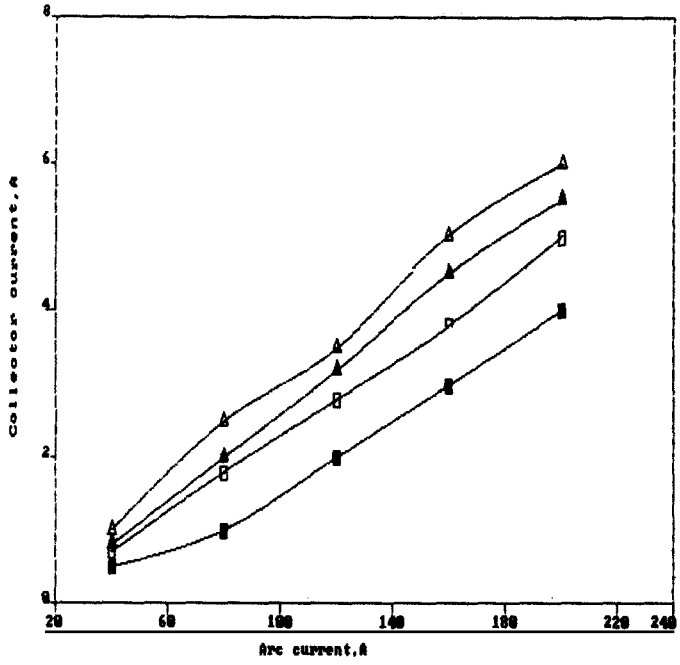

Fig. 2. Dependence of the ion flux to the collector placed in the anode region of the vacuum-arc on the electric current of the arc and the nitrogen pressure △ $p = 3 \times 10^{-4}$ hPa; ▲ $p = 5 \times 10^{-4}$ hPa; □ $p = 8 \times 10^{-4}$ hPa; ■ $p = 2 \times 10^{-3}$ hPa.

retaining magnetic field, taking the shape of the retaining magnetic field configuration and diffusing across the lines with the Bohm diffusion coefficient $D_B \approx Te/B$ [6]. The plasma concentration rises with the magnetic field strength.

The spreading of the plasma in the case of the vacuum arc column was proved experimentally in ref. 7.

The Thermion complexes comprise electric-arc evaporators with a linear cathode ensuring the uniform (on average) distribution of the plasma flux density when depositing coatings onto components of great length (Fig. 3). To produce flow-free electric-arc coatings, the plasma source is placed on a special electromagnetic plasma-guide-separator so that the working evaporating cathode surface does not enter the region of direct visibility from the substrate surface. During the source operation, the vacuum-arc plasma flux deviates by 90° along the lines of the toroidal magnetic field of the plasma-guide in the direction of the substrates, and macroparticles, the drop phase of the cathode erosion products, are trapped at diaphragms on the walls of the plasma-guide [8]. A system with radial flux is also used in which plasma flows out along the lines of the magnetic field produced by axially symmetric oppositely connected magnetic coils (Fig. 4). In this case the plasma source is placed on the axis of one of the coils and the substrates are placed axially

Fig. 3. The linear vacuum electric arc evaporator with titanium cathode of area $100 \times 400\ mm^2$, $I_c = 350$ A. A luminescent trace of the vacuum arc cathode spots is visible.

symmetrically on a carousel substrate-holder which ensures their rotation around the axis of the working chamber and around their axes.

In the electron-beam evaporator, a gas-discharge electron-beam gun with a cold cathode is used, ensuring that the evaporator can be used with plasma-forming gas pressures in the range 10^{-2}–10^{-5} hPa. The electric current in the gun is regulated within the limits of 0.1–1.0 A by a pressure change in the gas-discharge chamber.

The r.f. voltage is applied to the substrate-holder in the Thermion installation from a generator with frequency $f = 1.76$ MHz and maximum

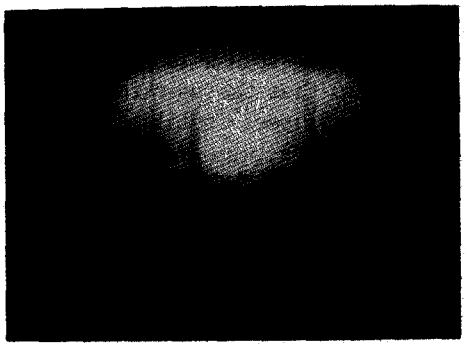

Fig. 4. The radial source of gas-metal plasma.

vibrational power of 25 kW. Simultaneously, the self-polarization potential is kept within 50–1500 V.

The Thermion installations are provided with a system of radiation-thermal heating with tungsten-wire resistive heaters which maintain the temperature of the substrates during coating in the range 150–1100 °C. This temperature is measured by an IR pyrometer. A cooling system allows the substrates to be cooled quickly (by a program) to 100–150 °C by forced gas convection in a pressure interval 10^{-2}–10 hPa. The installation is also fitted with a four-channel system providing metered gas supply with maximum flow rates in the channels of 50–200 cm^3 min^{-1}.

The plasma state is controlled in the Thermion by emission spectroscopy and by Langmuir wall probes operating in ion saturation mode [9, 10].

The thickness of the coating is controlled during deposition by registering the characteristic X-ray radiation induced by a diagnostic electron beam.

A system of automatic (programmed) control allows programmed technological cycles involving up to 20 stages of vacuum-plasma treatment to be carried out.

A study of the chemical interaction and the elemental composition of carbon coatings was carried out using Auger electron spectroscopy (AES), X-ray photo electron spectroscopy (XPS), ultrasoft X-ray emission spectroscopy (USXES), secondary-ion mass spectrometry (SIMS) and IR spectroscopy. When the distribution of elements across the thickness and the composition of the interface were studied by AES and XPES, the samples were first etched with an Ar^+ ion beam.

The microgeometry of sample surfaces was studied using a Talysurf-5M120 profilometer, a Neophot-2 optical metal-microscope, and a Camscan scanning electron microscope.

The strain properties of coatings were estimated using two methods of testing: hardness measurements on Knoop pyramid indents under different loads; measurement of strain properties using the diagram of Vickers pyramid penetration.

3. Results and discussion

3.1. The interaction of i-C coatings with the substrate surface

We studied i-C coatings deposited onto polished substrates of different materials by deposition from a flow of carbon vacuum electric-arc plasma with macroparticles removed. The energy of the carbon ions was in the range 50–500 eV during the deposition at a temperature not higher than 150 °C on the substrates. When the ions interacted with substrate atoms, chemical reactions which produced carbon compounds, radiation-stimulated diffusion of atoms of carbon and the substrate, and cascade mixing occurred.

On the surface of carbon film deposited onto a titanium substrate, carbon 1s electrons in a layer of carbon impurities have a binding energy of 286.0 eV. After etching with Ar^+ ions for 30 s, removing a layer 50–100 Å thick, in

TABLE 1

Parameters of chemical interactions of carbon with substrate material

Reaction numbers	Reaction of carbon with substrate atoms	ΔG (cal kg^{-1})	Method of study	Presence of carbides at interface
1	$Si + C = SiC$	−71	AES, XPS	+
2	$2Al_2O_3 + 3C = Al_4C_3 + 3O_2$	2960	AES, XPS	−
3	$2Al_2O_3 + 9C = Al_4C_3 + 6CO$	3300	AES, XPS	−
4	$2Al_2O_3 + 6C = Al_4C_3 + 3CO_2$	1775	AES, XPS	−
5	$Ti + C = TiC$	−188	XPS	+
6	$3Fe + C = Fe_3C$	20	XPS	−
7	$Zr + C = ZrC$	−194	AES	+
8	$Nb + C = NbC$	−139	AES	+
9	$2Nb + C = Nb_2C$	−192	AES	+
10	$Ta + C = TaC$	−145	AES	+
11	$2Ta + C = Ta_2C$	−194	AES	+

addition to the main peak with energy 285.2 eV, a peak with energy 282.0 eV appeared, indicating the presence of titanium carbides at the interface [11]. The amount of carbon bonded into the titanium carbide is three times less than the total carbon content at the interface. The results of similar studies of chemical interactions of i-C films with substrates made of different materials are given in Table 1. Estimates of the change in Gibbs free energy for typical solid-phase interactions between the carbon coating and substrate atoms obtained using standard thermodynamic functions are also given. For carbon coatings, the thermodynamic values corresponding to glass-like carbon were used because the structure of the deposited carbon films is closest in the type of chemical bond, to glass-like carbon [12, 13].

As is seen from the table, for reactions 1, 5 and 7–11, $\Delta G < 0$, showing that these reactions can occur at deposition temperatures.

Detailed calculation of the thermodynamically equilibrated composition of a transitory carbon layer and several metals has shown that even when oxygen and nitrogen are present, the formation of carbides is possible for chromium substrates at $T \gtrsim 750$ °C, for zirconium substrates at $T \gtrsim 1200$ °C, and for titanium substrates at $T \gtrsim 900$°C.

According to the data from ref. 14, when carbon interacts with a metal surface in vacuum, carbides are formed on substrates ranging from tungsten at $T \gtrsim 1400$ °C, molybdenum at $T \gtrsim 1200$ °C and tantalum at $T \gtrsim 1000$ °C. Estimations show that these temperatures can be reached over small (of the order of several interatomic distances) regions close to the site of carbon ion implantation into the surface of the growing film [15].

By etching the surface of the films layer by layer with Ar^+ ions, profiles of the distribution of elements at the interfaces with carbon films were obtained. As is seen from Fig. 5, the interface of a carbon coating on aluminium contains carbon (binding energy 272 eV), oxidized aluminium (51 eV), non-oxidized aluminium (68 eV) and oxygen (532.2 eV). In all the samples

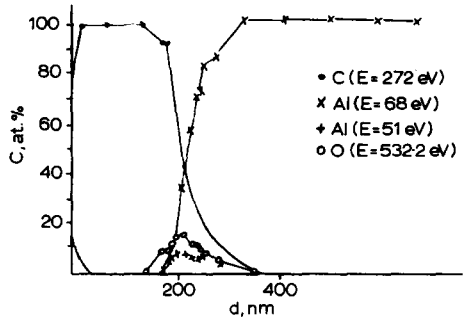

Fig. 5. The interface of a carbon coating on aluminium.

studied, the profiles of carbon and aluminium oxide in the interface region terminated simultaneously. Non-oxidized aluminium was observed in the transitional region before the drop in aluminium oxide content occurred. This fact shows that during the initial stages of coating formation, carbon, aluminium oxide and aluminium mix together, the aluminium oxide penetrating deeper into the forming film than aluminium.

The thermodynamic calculation (Fig. 6) confirmed the thermodynamic stability of aluminium oxide and nitride in the carbon environment at temperatures typical for the synthesis of i-C coatings.

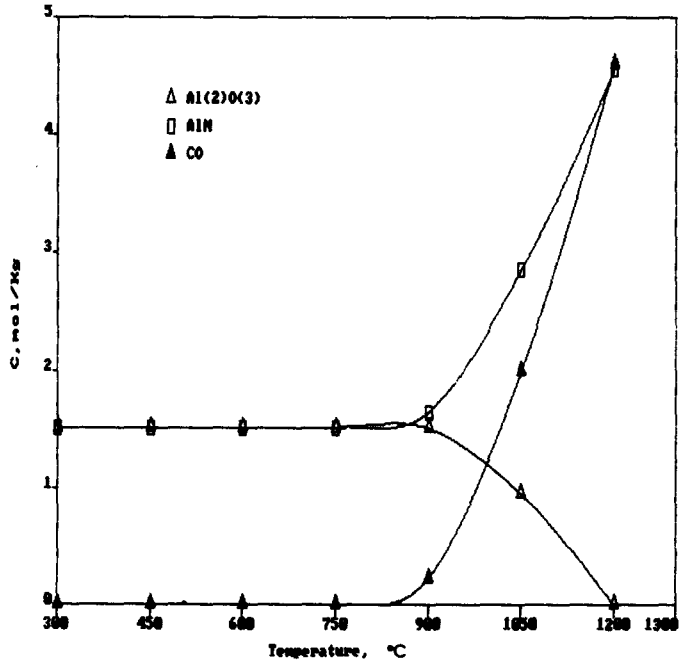

Fig. 6. The dependence of the concentrations of components of a thermodynamically balanced mixture of composition Al–C–O–N on temperature at $p = 10^{-3}$ hPa.

It also indicated the presence of considerable concentrations of carbon oxide which is proved by the results of IR spectroscopy. Carbon oxides can penetrate into the growing film from the plasma flux where they are formed by the interaction of residual air oxygen, and oxygen contained in the graphite cathode, with carbon atoms at the high-temperature regions of the working surface of the cathode. This is confirmed by the dependence of the radiation intensity of the line C1 (2478 Å) and the band CO^+ (4273.3 Å) on the electric current of the carbon vacuum-arc, as shown in Fig. 7.

Figure 8 shows the relationship between the thickness of the i-C coating and the transitional region between it and the aluminium substrate, and the potential of the substrate self-polarization (a value close to the energy of the deposited ions) and the time of film formation. The size of the transition region grows both with increasing carbon ion energy and increasing time of film formation. Taking into account that the integral temperature of the substrates did not exceed 100–150 °C during deposition, it is possible to suggest that the formation of the transition zone is affected by radiation-stimulated diffusion, cascade mixing and intensive acoustic vibrations induced in the surface layer by ion bombardment along with thermodiffusion. The existence of thermodiffusion is proved by the fact that growth of the transitional region continues even after the external film boundary is shifted away from the boundary of the transitional region to a distance which exceeds the maximum length of the collision cascade.

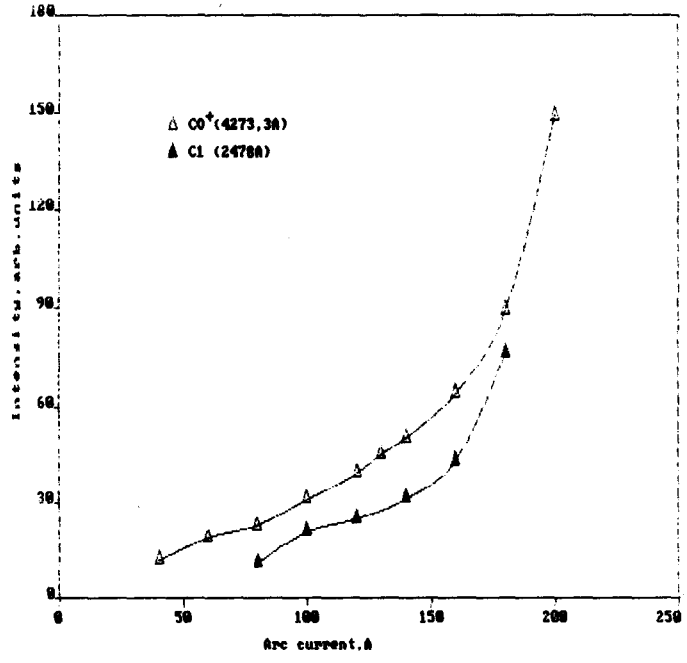

Fig. 7. The dependence of the radiation intensity for line C1 (2478 Å) and band CO^+ (4274.3 Å) on the electric current of the carbon arc ($p = 10^{-5}$ hPa).

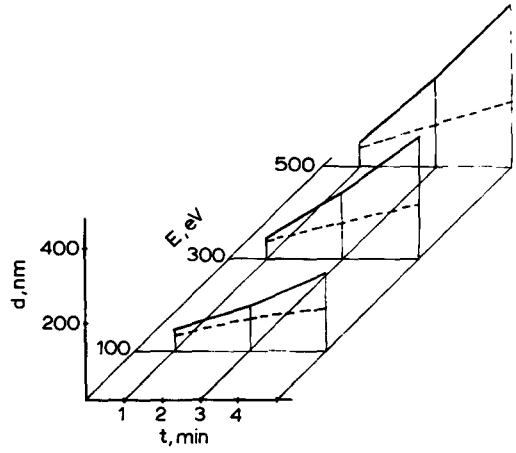

Fig. 8. The dependence of the i-C film thickness and the width of the interlayer between the film and the aluminium substrate on the self-polarization potential of the substrates and the time of deposition.

To describe the kinetics of the formation of the transitional region during the initial stage of i-C coating synthesis, a simple physical model taking into account the diffusional and cascade mixing, and the selective spraying and recycling of atoms in the plasma layer adjoining the substrate [16], was constructed. Assuming a number of simplifications, the equation describing the distribution across the thickness ξ at time t of the relative carbon concentration $\rho_1(\xi, t)$, can be reduced to the form:

$$\frac{1}{h^2}\frac{\partial \rho_1(\xi,t)}{\partial t} = \frac{\partial}{\partial \xi}\left\{g\frac{\partial \rho_1(\xi,t)}{\partial \xi} + [N(1-\kappa)((S_{01}-S_{02})\rho_1(0,t)+S_{02}) - \psi(t)]\rho_1(\xi,t)\right\} \quad (1)$$

where the depth ξ is expressed in units of the distance between the atomic layers h, D is the diffusivity, N is the sprayed (and deposited) flux of atoms and ions of carbon, $g \equiv D/h^4 + u + (NS_{01}/2)(1+\kappa)$, S_{01} is the coefficient of carbon self-spraying, S_{02} is the coefficient of spraying of the substrate material, the coefficient of recycling κ is defined by the ratio of the number of atoms returned to the surface and the total number of atoms sprayed; the concentration of atoms of the base is related to the concentration of atoms of the coating by the equation $\rho_2(\xi, t) = 1 - \rho_1(\xi, t)$; $u = u(\xi)$ is the number of exchange transfers of atoms of different kinds from neighbouring atomic layers.

Figure 9 shows the distributions of aluminium, iron and titanium atoms in the transitional layer of the i-C coating which were calculated by solving eqn. (1) with varied parameters of diffusional and cascade fluxes of atoms. The qualitative conformity of the calculations with experimental results allows us to predict the actual form of the concentration profile of atoms in the transitional layer under various coating conditions by using this theory.

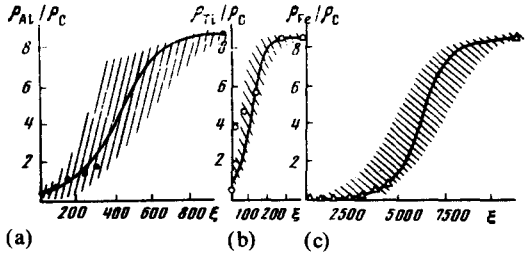

Fig. 9. The distribution across the depth ξ of the ratio ρ between the concentration of substrate atoms and the concentration of carbon atoms when depositing i-C coatings: (a) aluminium, (b) titanium and (c) iron. The points in the diagram are the results of experimental studies [11, 12, 17], the curves are model (1) based calculations. The cross-hatched areas are variations of theoretical results following a change in input parameters over the interval of confidence.

Summing up the results of the above study of the region where the carbon coating interacts with substrates of different materials, it is possible to conclude that the size of the interaction region does not exceed 0.5 μm for all the materials studied. The contribution of chemical interaction to the formation of the structure of the region is relatively small. The definitive effect on the distribution of elements in the interaction region is exerted by the diffusional and cascade processes of mixing atoms which depend on the substrate temperature, the kinetic energy of the deposited particles, the characteristics of the plasma layer adjoining the substrate, and the substrate material.

The character of elemental distribution in the transitional i-C–substrate region is related to the adhesion of the i-C coatings. Thus, the adhesion of i-C coatings on titanium substrates was worse than that on iron-substrates, in spite of the existence of chemical interactions between the i-C coating and the titanium substrate. The best adhesion was observed when i-C coatings were deposited onto substrates of aluminium coated with a layer of aluminium oxide, or onto sapphire (Al_2O_3) substrates.

This is illustrated in the photograph of the region where the i-C coating scales on aluminium after heating the aluminium substrate to the melting temperature (Fig. 10). It is interesting that the adhesion of the i-C coating on non-oxidized aluminium is considerably lower; this is confirmed by measurements of i-C coatings deposited onto layers of aluminium just deposited in vacuum.

3.2. The formation of the surface microgeometry by the deposition of multilayer superhard coatings

The formation of the surface geometry under the action of plasma is governed by processes such as surface spraying by ion bombardment, condensation of gas–metal plasma, thermodiffusion and segregation in the subsurface layer etc. As a rule, these processes lead to an increase in surface roughness which sharply lowers the efficiency of the technology of vacuum-plasma strengthening.

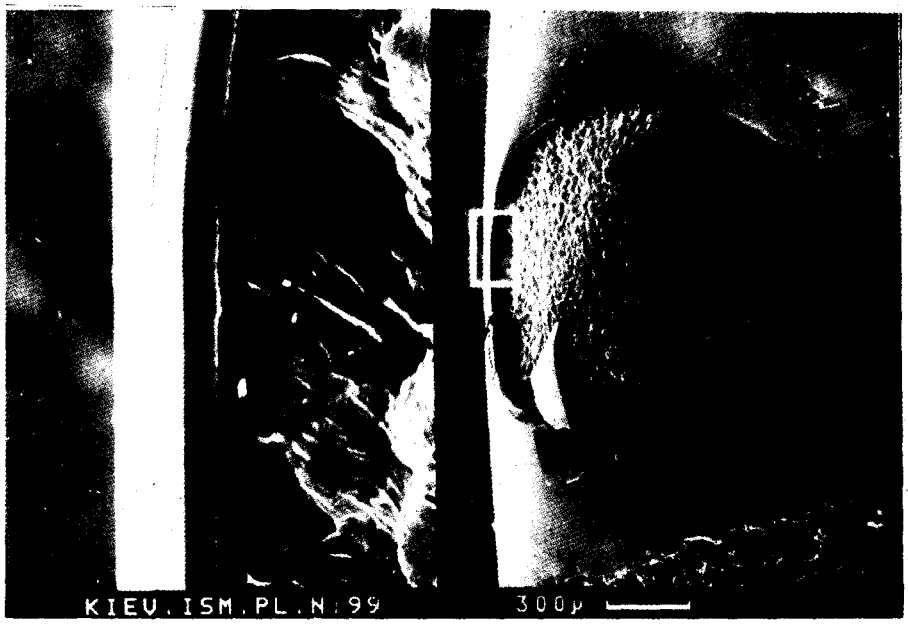

Fig. 10. A stretch of i-C coating on melted aluminium surface.

This particularly concerns the deposition of thin superhard coatings which only reveal their unique mechanical properties on smooth surfaces. Therefore, when developing the complex vacuum-plasma strengthening technology, special studies of the dynamics of the formation of surface relief during various stages of the process were carried out.

The study of the formation of surface relief during ion cleaning and deposition of the cermet underlayer was performed on samples of bases for hard memory disks used in Winchester type memory disk units. Bases for hard disks are made from aluminium alloy by microturning; they have a surface roughness $R_a = 0.015–0.035\ \mu m$, $R_p = 0.06–0.095\ \mu m$, $R_z = 0.055–0.1\ \mu m$ and $R_{max} = 0.09–0.15\ \mu m$. Improved surface roughness parameters ($R_a = 0.008\ \mu m$, $R_p = 0.04\ \mu m$) can be achieved by plating the aluminium surface after microturning with a galvanic NiP coating about 20 μm thick, followed by polishing.

When choosing a plasma medium for ion cleaning of surfaces before coating it was established that ion bombardment in Ar^+ plasma leads to a rapid rise in the surface roughness of aluminium owing to ion etching. It was possible to avoid this effect by using an atomic-pure titanium or nitrogen–titanium cathode-arc plasma for ion cleaning.

For Ti^+, N^+ and N_2^+ ions with energy less than or approximately equal to 1 keV, the coefficient of spraying does not exceed 0.1 atom per ion [19], which allows desorption and activation of the surface practically without spraying.

A study of the dynamics behind the formation of the surface microgeometry was carried out when depositing cermet TiN coatings from a flux of atomic-pure Ti–N_2 vacuum-arc plasma with the macroparticles removed (drop phase). The dependence of the basic surface roughness parameters at coating rates of about 1 μm h^{-1} are shown in Fig. 11. It is seen that at cermet sublayer thicknesses up to 0.5 μm, the surface roughness does not vary substantially.

Measurements of surface roughness parameters on magnetron titanium and chromium layers 3 μm thick deposited onto the surface of the aluminium hard disk base with a TiN vacuum-arc sublayer, have shown that surface roughness parameters of a magnetron layer are of relatively low magnitude, even when the layer thickness is considerable ($R_a = 0.035$ μm, $R_p = 0.137$ μm, $R_{max} = 0.569$ μm) which means that the method has potential for producing multilayer cermet coatings deposited before the final superhard i-C layer.

A study of the morphology of i-C coatings on substrates of different materials has shown that i-C films deposited from a flux of vacuum electric-arc plasma consist of disorderly disposed blocks of spherulites and whiskers having a substructure (Fig. 12). The deposition of whiskers, and the concentration and size of spherulites, are defined by defects and the substrate surface microgeometry as well as the duration of coating formation [17].

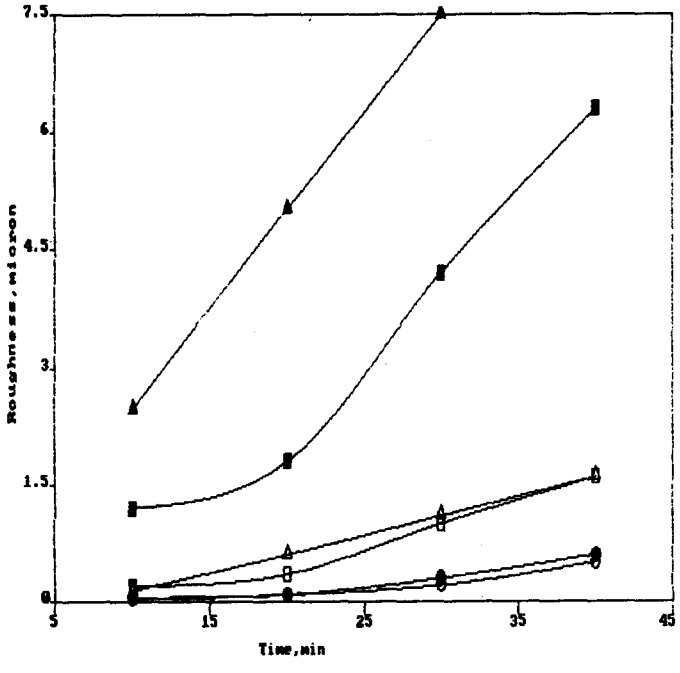

Fig. 11. The dependence of the roughness height parameters of TiN coatings on the coating thickness: △ thickness of cathodic-arc coatings with separation of droplets; ▲ thickness of coatings without separation; □ R_z for coatings without separation; ■ R_a for coatings without separation; ○ R_z for coatings with separation; ● R_a for coatings with separation.

Fig. 12. The i-C film on the surface of cemented carbide ($\times 2000$).

Spherulites may form two-dimensional turbostrate structures. At the same time, spherulites are predominantly located at sites of surface defects on the substrate which result from its preliminary mechanical machining. In these spherulites, which cover 10% of the substrate surface area, sulphur, calcium and chlorine impurities are found which are absent in the rest of the film; the concentration of other impurities in the spherulites exceeds their concentration in the rest of the film by 1–2 orders of magnitude. This can be attributed to two-dimensional condensation under the conditions of radiation-stimulated diffusion [11].

A study of the formation of surface microgeometry during separate stages of the complex technology of hardening steel surfaces was carried out on 40 samples of chrome steel, $10 \times 20 \times 5\ mm^3$, whose surface was first ground and polished to a surface roughness of $R_a = 0.011\ \mu m$, $R_p = 0.049\ \mu m$, $R_z = 0.047\ \mu m$, $R_{max} = 0.098\ \mu m$.

These samples were subjected to various stages of vacuum-plasma treatment. Values of the surface roughness are given in Table 2 where it is shown that deposition of the i-C sublayer exerts hardly any influence on the surface microrelief. At the same time, nitriding combined with the presence of the TiN-sublayer, increases the surface roughness of the steels and the TiN coating produced by direct deposition makes the surface unfit for use as a sublayer for i-C coatings owing to the presence of titanium drops produced by erosion of the cathode. Deposition of the i-C sublayer ($\delta \lesssim 0.5\ \mu m$) on the hardened surface of a part being treated without any significant changes in the surface roughness provides optimal conditions for the further deposition of diamond or diamond-like coatings having the highest possible adhesion.

3.3. Mechanical properties of superhard coatings

To study the strain properties of multilayer samples with superhard coatings by the hardness test method, the characteristics of deformation of samples of different materials with i-C coatings were first investigated, allowing a quantitative estimation of the properties of double-layer samples since the hardness relates to the yield strength ($H = \beta\sigma\rho$) and correlates with the elastic modulus. In the case of thin films (when the elastic strain region

TABLE 2

Values of the roughness height parameters under different conditions of vacuum-plasma treating of steel

Condition	Vacuum-plasma treatment	R_a (μm)	R_p (μm)	R_z (μm)	R_{max} (μm)
1	Ion nitriding to 30 μm followed by TiN sublayer 0.5 μm thick deposited from separated cathode-arc plasma	0.06	0.208	—	0.317
2	Direct deposition of 5 μm thick TiN coating from cathode-arc plasma (without separation)	0.475	3.032	1.094	4.726
3	Deposition of 0.5 μm thick i-C coating 150 eV	0.022	0.098	0.062	0.266
4	Deposition of 0.5 μm thick i-C coating 500 eV	0.039	0.208	—	0.111
5	1 and 3	0.053	0.198	—	0.308
6	1 and 4	0.066	0.208	0.137	0.406

exceeds the film thickness), however, the properties of the substrates will substantially affect the results of measurements [17].

Hardness measurements on i-C coatings of different thicknesses deposited onto the same substrate (copper) allowed us to establish the following peculiarities of deformation. At low loads, a fully recovered indent with some fracturing in the region of contact between the sample and indenter is observed. At large loads, the film fractures in a brittle way, taking on the shape of the plastically deformed area of the substrate. The load value P_c at which the transition from elastic contact to plastic indent occurs increases with film thickness. Thus the film hardness can be evaluated when the region of elastic–plastic deformation does not exceed the film thickness.

When indenting films of the same thickness deposited onto substrates of different materials (aluminium, steel, cemented carbide, diamond) the regularities are similar, *i.e.* with increasing elastic modulus of the substrate, the load value P_c at which the transition from elastic contact to plastic indent occurs also increases.

The microhardness study of the i-C film on diamond has shown that with increasing load from 0.98 to 9.8 N, there is a reduction in hardness from 40 to 25 GPa.

When the load is increased further, brittle fracture of the coating is observed over an area considerably larger than that of the contact region under the indenter (Fig. 13).

To evaluate quantitatively the mechanical properties of i-C films on substrates of different materials, diagrams of penetration were plotted using

Fig. 13. The region of the brittle indent fracture on an i-C coating 5 μm thick on diamond.

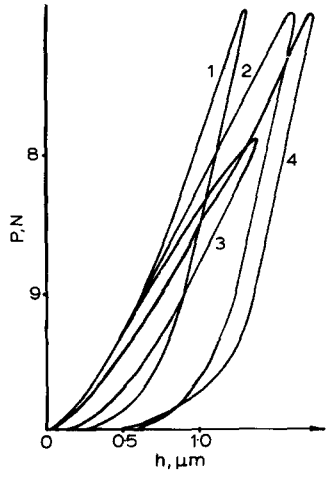

Fig. 14. Diagram of indenter penetration into the surface of samples of diamond (curve 1), cemented carbide WC-2 (curve 2) and copper (curve 3) with i-C coatings 5–7 μm thick, and the surface of WC-2 without coating (curve 4).

the coordinates of load and indenter penetration depth. Analysis of the penetration diagram for i-C film on copper, cemented carbide and diamond gives the basis for confirmation of the above-mentioned effects of substrate properties on the unrecoverable hardness.

It is seen from Fig. 14 that the depth of indenter penetration reduces with increasing substrate hardness, *i.e.* the value of unrecoverable hardness

TABLE 3

Modulus E and the hardness H_μ of i-C coating on different substrates

Number	Substrate material	E (GPa)	(H_μ) GPa
1	Diamond	429	28.84
2	Copper	207	13.04
3	Cemented carbide WC-2	515	21.89
4	Glassy carbon without i-C coating	12.1	1.06

increases. As the load increases to $P = P_c$, the depth of penetration is practically the same and the branches of loading coincide. However, at loads lower than P_c as shown above, plastic deformation is absent and the i-C coating reveals elastic properties only. Therefore, the definition of hardness adopted using the indent depth is not valid over this range of loads. In the region lying above P_c in the diagram, the effect of the substrate is clearly evident, so the unrecoverable hardness will be higher the harder the substrate material is (see Table 3 [17]).

According to the diagrams of indenter penetration into cemented carbide WC-2 and the sample of WC-2 with i-C coating, the loading curves to P_c for both samples are equal. Then the loading curve of the sample with the film becomes higher than that of WC-2. This can be attributed to the fact that after fracture of the film, the substrate deforms but the fractured film modifies the pressure distribution under the indenter which is reflected in the diagram. The unloading curves are parallel, *i.e.* during unloading WC-2 recovers but the fractured film does not.

The studies performed have not only theoretical but also practical value because they allow the deformation properties of a two-layer sample, substrate–i-C coating, to be evaluated. In particular, it follows from the results obtained that the critical load P_c at a fixed i-C coating thickness will be higher the harder the substrate is. Consequently, it is possible to expand substantially the range of loads over which the i-C coating will reveal purely elastic properties by increasing the substrate hardness. These properties, along with high corrosion resistance and low friction coefficient, define a range of applications of i-C coatings as strengthening coatings for tools and friction components operating under abrasion–corrosion wear conditions at low contact loads. This is illustrated by the following examples.

Table 4 gives test results for steel and cemented carbide drills when drilling printed circuit boards made from foiled glass-fabric resin laminate and graphite blocks. Here, drills without coatings and drills with i-C and i-TiN coatings deposited from cathode electric-arc plasma flux free of macroparticles are compared. It is seen that the increase in coefficient of resistance K_s for steel drills with the coating is about ten times greater than that for cemented carbide drills. However, in absolute values of the number

TABLE 4

Results of comparative testing of drills with ion-plasma coatings

Number	Material of drill base	Diameter of drill (mm)	Type of coating	Number of holes satisfying the state standard requirements	Coefficient of the increase in strength K_s
1	HSS steel	1	—	10	1
2	HSS steel	1	i-C	120	12
3	Cemented carbide WC6M	1	—	3730	1
4	WC6M	1	i-TiN	4300	1.16
5	WC6M	1	i-C	5900	1.58
6	WC6M	1	i-C (after resharpening)	4662	1.25
7	HSS steel	10	—	100	1
8	HSS steel	10	i-C	430	43

For samples 1–6, the material treated was bases for printed circuit boards made of glass fabric resin foil with protective lac coating. For samples 7 and 8 the material treated was graphite.

of holes drilled, cemented carbide drills by far exceed coated steel drills. The increase in resistance after deposition of the i-C coating is more than 40% higher than after depositing i-TiN coatings. It should be noted that coatings deposited by the above method reveal a fine crystalline (close to amorphous) structure and are like i-C coatings in their mechanical properties. They also have a high microhardness under low loads and with an increase in load they fracture in a brittle way. In contrast to i-C coatings, i-TiN coatings almost completely lack the region of elastic behaviour. Therefore, the wear on drills with i-TiN coatings under conditions where the abrasion–corrosion interaction is decisive and the contact loads are low, exceeds considerably the wear on drills with i-C coatings.

It should be noted for comparison that i-C coatings are impractical and inefficient for steel drilling, whereas i-TiN coatings give very good results.

i-C coatings were also used for strengthening special cutter-combs for threading graphite electrodes. Two types of cutters were tested; cutters from low carbon steel tempered to a hardness of HR_c 54 and cutters from cemented carbide of WC8 grade. Cemented carbide WC8 cutters without coating were tested simultaneously for comparsion of the test results obtained for these cutters.

The wear on the cutters during testing is characterized by a change in their geometric dimensions: the dimension h_f on the cutting face and h_b on the clearance face. The test results are given in Fig. 15 where the number of electrode machines is shown on the abscissa. It is seen that at the initial stage, while the i-C coating is retained, the wear rate on steel cutters is less

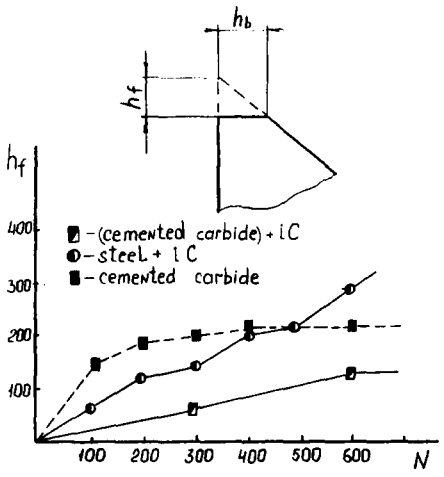

Fig. 15. Results of comparative testing of cutters with i-C coatings.

than on cemented carbide cutters which can be attributed, as it was in the first case, to the high abrasive resistance of i-C coatings. When depositing i-C coatings onto cemented carbide cutters, their resistance is enhanced by around 20%, which is in agreement with the results obtained in testing drills. It should be noted that the deposition of i-TiN coatings had practically no effect in this case.

At the same time, the deposition of ion cermet coatings as sublayers between the base and the i-C film improves the adhesion of the i-C coating to the base and increases the hardness of interlayer between the i-C coating and the base, which may result in an increase in the load at which the substrate strain no longer influences the coating resistance.

The effects of a cermet sublayer on the mechanical properties of coatings were modelled on samples of bases for hard aluminium memory disks.

Samples with titanium and chromium up to 5 μm thick deposited directly onto the aluminium surface by the magnetron method, and with a TiN sublayer deposited from a flux of vacuum-arc plasma free of macroparticles, were studied. Some of the samples were coated with a hard galvanic sublayer of NiP with $H_\mu \approx 800$ kgf mm^{-2} before vacuum-plasma deposition (see section 3.2). The surface microhardness of the samples with multilayer coatings was measured under different loads from 10 to 500 gf.

Figure 16 shows the dependence of the penetration pressure on the depth of the indenter penetration, $P = f(h)$. For a monolithic continuous material the dependence $P = f(h)$ on a logarithmic scale is close to linear [18].

Samples with titanium and chromium coatings on aluminium show the relationship $P = f(h)$ (open and closed triangles, Fig. 16) consisting of two linear stretches. The boundary of these stretches is the depth of penetration commensurable with the coating thickness. This indicates that the aluminium substrate has a substantial effect on the results of the hardness

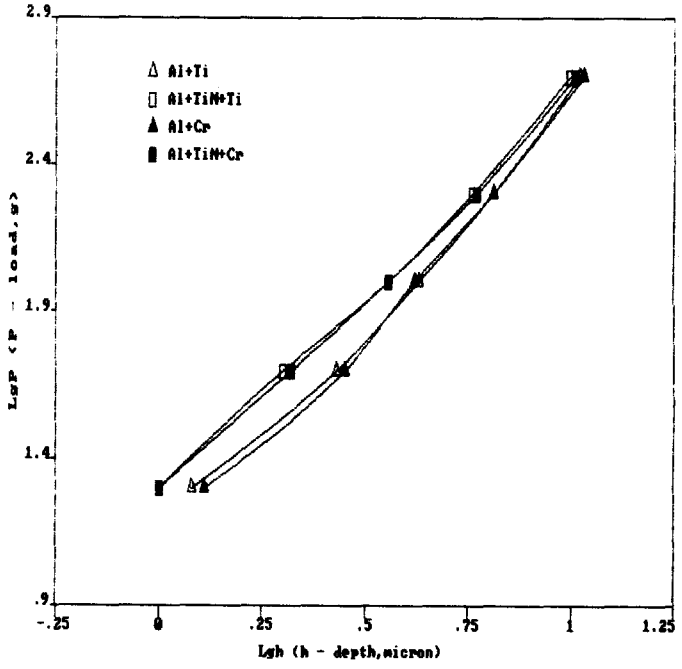

Fig. 16. The dependence of the penetration pressure on the depth of indenter penetration, $P = f(h)$.

measurement at large loads. Therefore, under these conditions, the hardness of the samples is close to that of aluminium.

Samples with titanium and chromium coatings deposited onto aluminium using a TiN sublayer 0.5 μm thick do not show a notable break in the dependence $P = f(h)$ (open and closed rectangles, Fig. 16). This means that the TiN layer "screens" the effect of the substrate on the coating hardness. In this case the surface microhardness value is more than two times higher than with the TiN sublayer.

For samples with an NiP sublayer 8–10 μm thick, the thickness of the coatings is commensurable with the depth of the indenter penetration even at maximum loads. The dependence $P = f(h)$ for these samples shows an inverse bend attributed to the effect of the thick NiP sublayer. Over the entire range of loads, the hardness of these samples is considerably higher than that of samples without the NiP sublayer.

Summing up all the above, it is possible to say that an increase in thickness of the interlayers of cermet coatings, and an increase in their number, lead to substantial enhancement of the hardness and lessen the effect of the base material on the deformation properties of the surface. Simultaneously, the choice of material for the cermet layer carrying the last i-C layer must be made taking into account its adhesion to the i-C coating and its surface roughness.

Acknowledgments

This work made use of developments fulfilled under the Complex Programme for Research and Technical Progress of members of Comecon by a team including specialists from the Ukraine, Estonia, Belorussia, R.S.F.S.R., Poland, Romania and East Germany.

The authors express their deep thanks to the leading coordinator of the Protective Coatings subprogramme of the Complex Programme of Comecon, Professor K. A. Yushchenko, for financial support and constant attention to the work.

The authors are grateful to Dr. D. Fabian of the Machine-tool Building Institute, East Germany, Dr. A. Sokolowska of Warsaw Polytechnical Institute, Professor Z. Has and Dr. S. Mitura of Lodz Polytechnical Institute, Dr. M. Druga and licensed engineer A. Radu of the Metallurgy Institute, Romania, Dr. T. Thomson of the Institute of Thermoelectrophysics, the Estonian Academy of Sciences, Dr. A. Masurkevich of the Smorgon optical machinery plant, Dr. E. Petrov of the All-Union Institute of HF-electric currents as well as their colleagues for their participation in the development of the Thermion installation modules and in technological studies and fruitful discussions.

The authors also express their gratitude to the members of the group of vacuum plasma technology at the Institute for Superhard Materials of the Ukrainian Academy of Sciences for taking part in the experiments, the scientific workers of the Institute, Dr. A. Smekhov, Dr. E. Pugach, Dr. V. Malnev, Dr. A. Orap, Dr. N. Stakhniv and their colleagues for carrying out experimental studies of the coating properties, and Dr. Ya. Filippov of the All-Union Scientific Society for financing the work.

References

1 I. I. Aksenov, V. G. Padalka, V. E. Strel'nitsky and V. T. Tolok, *Sverkhtverdye Materialy, I* (1979) 25.
2 T. Yoshioka, O. Imai, H. Ohara, A. Doi and N. Fujimori, *Surf. Coatings Technol., 36* (1988) 311.
3 G. Graff, *Diamonds Find New Setting, High Technology, April* (1987) 44–47.
4 A. S. Vereshchaka and I. P. Tretyakov, *Cutting Tools with Wear Resistant Coating,* Mashinostroyenie, Moscow, 1986 (in Russian).
5 *Thermion,* Institute for Superhard Materials of the Ukrainian S.S.R., Academy of Sciences, Kiev, 1989 (in Russian).
6 F. Chen, *Introduction to Plasma Physics and Controlled Fusion,* Vol. 1, Plenum, New York, 1984, p. 186.
7 V. I. Gorokhovsky, V. P. Yelovikov, P. L. Lizunov and S. A. Pantyukhin, *Teplofiz. vys. Temp., 26* (1988) 239.
8 I. I. Aksenov, V. G. Padalka and V. M. Khoroshikh, *Formation of Metal Plasma Flows* (Review), TsNIIatominform, 1984 (in Russian).
9 V. I. Gorokhovsky, G. N. Kurtynina and D. K. Otorbayev, *Chem. High Energies, 23* (1989) 356.
10 V. I. Gorokhovsky and V. P. Yelovikov, *Zh. Tekh. Fiz., 57* (1987) 2267.

11 V. G. Aleshin, V. I. Gorokhovsky, A. A. Smekhnov and M. G. Chudinov, in N. V. Noviko (ed.), *Surface and Thermo-Physical Properties of Diamond*, Institute for Superhard Materials of the Ukrainian S.S.R., Kiev, 1985, p. 28 (in Russian).
12 V. G. Aleshin, V. I. Gorokhovsky, V. G. Malogolovets, A. A. Smekhnov and B. A. Uryukov, *Proc. Int. Scientific Meet. of the COMECON Countries on Vacuum Processes for Plasma-Aided Application of Wear Resistant Coatings on Tools and Machine Parts, Warsaw, 1987*, Warsaw Polytechnical Institute, Warsaw, 1987, p. 8.
V. I. Gorokhovsky, A. G. Zhiglinsky, V. V. Kuchinsky, V. A. Fomichev and A. S. Shulakov, *Proc. Int. Scientific Meet. of the COMECON Countries on Vacuum Processes for Plasma-Aided Application of Wear Resistant Coating on Tools and Machine Parts, Warsaw, 1987*, Warsaw Polytechnical Institute, Warsaw, 1987, p. 12.
13 I. Barin and O. Knake, *Thermochemical Properties of Inorganic Substances*, Springer, Berlin, 1973, p. 921.
14 L. I. Maissel and R. G. Glang (eds.), *Handbook of Thin Film Technology*, Vol. 1, Springer, Berlin, 1970.
15 G. Reiss, C. Schürer, V. Ebersbach, K. Bewilogna, K. Breuer, H.-I. Erler and C. Weissmantel, Herstellung und Untersuchung von i-Kohlenstoffschichten, *Wiss. Z. Tech. Hochsch. Karl-Marx-Stadt, 22* (7) (1980) 676.
16 V. G. Aleshin, V. I. Gorokhovsky, V. V. Dunayev, A. G. Zhiglinsky, V. V. Kuchinsky, A. A. Smekhnov, B. A. Uryukov and E. P. Sheikin, *Fiz. Khim. Obrab. Mater.*, (6) (1987) 69.
17 B. A. Uryukov, V. G. Aleshin, E. A. Pugach, V. I. Gorokhovsky, V. I. Malniev and A. A. Smiechnov, *Arch. Nauk. Mater.*, *7* (1986) 105.
18 A. M. Terkovsky, V. P. Alekhin and M. Kh. Shorshorov, in M. M. Kruschchov (ed.), *Novelty in Microhardness Testing*, Nauka, Moscow, 1974, p. 71 (in Russian).
19 R. Berisch (ed.), *Sputtering by Particle Bombardment*, Vol. 1, Springer, Berlin, 1981, p. 227.